Supporting Information for

"Magnetospheric and solar wind dependences of coupled fast-mode resonances outside the plasmasphere"

M. O. Archer, [1,2]

M. D. Hartinger, [3]

B. M. Walsh, [4]

V. Angelopoulos, [5]

[1]School of Physics & Astronomy, Queen Mary University of London, London E1 4NS

[2]Space & Atmospheric Physics Group, Blackett Laboratory, Imperial College London, London, SW7 2AZ, UK.

[3]Electrical and Computer Engineering Department, Virginia Tech, Blacksburg, VA, USA.

[4]Department of Mechanical Engineering and Center for Space Physics, Boston University, Boston MA, USA.

[5]Department of Earth, Planetary and Space Sciences, University of California, Los Angeles, CA, USA.

Contents

Introduction

This supporting material shows the same analysis techniques used for the dawn and dusk sectors applied to noon, where cFMR are less likely to occur.

Corresponding author: M. O. Archer, m.archer10@imperial.ac.uk

Figure S1.

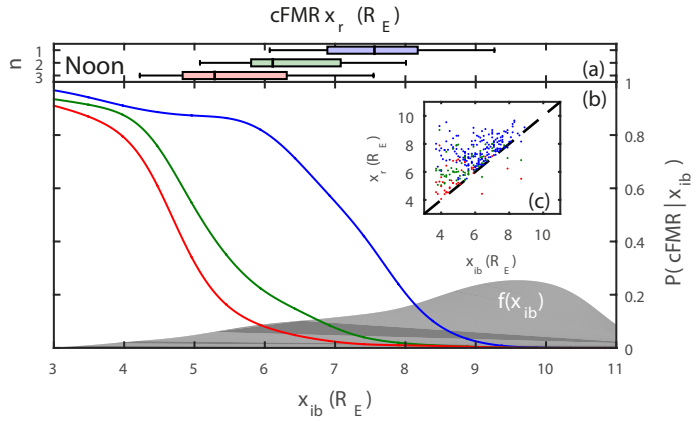

Possible occurrence of cFMR (n = 1–3 in blue, green, red) in the noon sector as a function of the inner boundary location. The grey shaded area represents the distribution of inner boundary locations. Box plots of resonance locations are displayed where whiskers represent 95% of the data (a). Scatter plots of resonance against inner boundary locations are shown inset (c).

Figure S2.

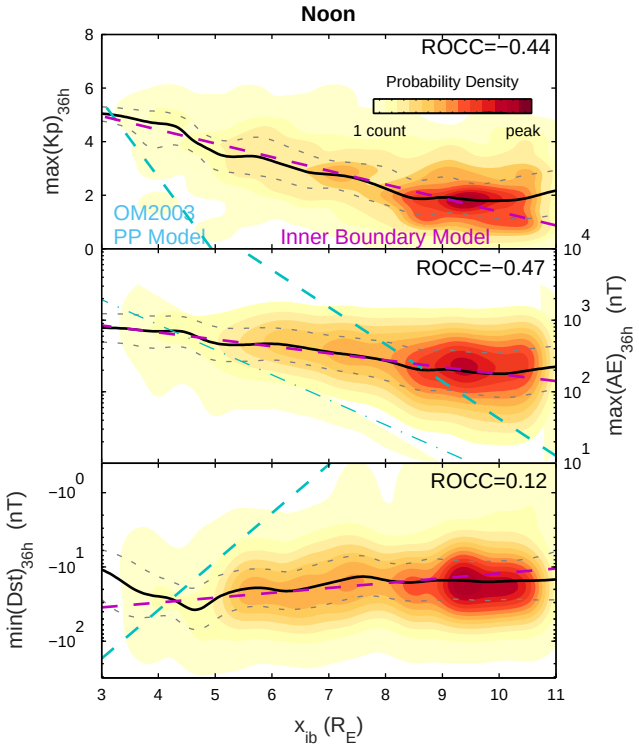

Linearly-spaced contours of the distribution of inner boundary locations against the Kp (top), AE (middle), and Dst (bottom) indices at noon. Lines show the medians (solid) and interquartile ranges (dotted) with inner boundary location along with the *O'Brien and Moldwin* [2003] plasmapause model (turquoise dashed; MLT independent model also shown for AE as dot-dashed line) and our linear fit (purple). Rank order correlation coefficients are also displayed.

Figure S3.

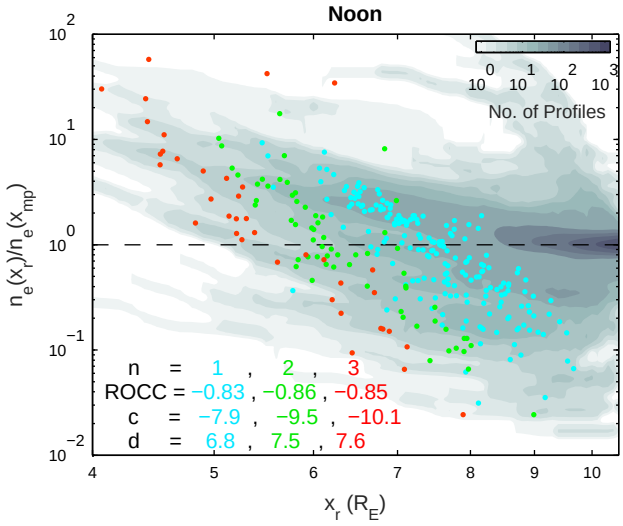

Relationship between noon sector cFMR resonance locations (n = 1–3 in blue, green, red) and ratio of the density at the resonance to that near the magnetopause. The full distribution of outer magnetospheric density ratios is shown as contours. Rank order correlation and power law fit coefficients are also displayed.

Figure S4.

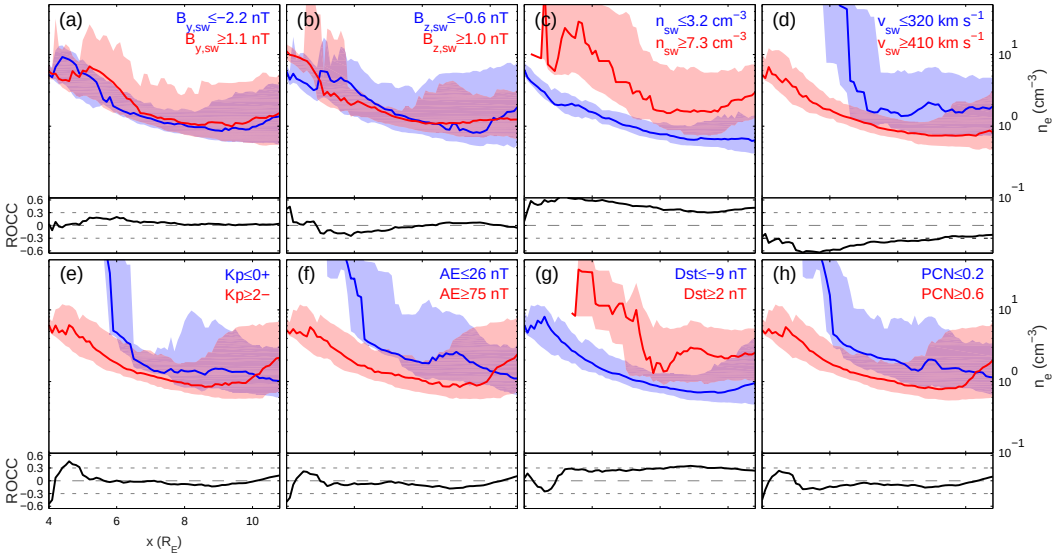

Dependence of density profiles in the noon sector on solar wind conditions (a–d) and magnetospheric activity indices (e–h), displaying the upper (red) and lower (blue) quartiles. Solid lines and shaded areas represent the medians and interquartile ranges over these subsets. Lower panels show the rank order correlation coefficient with radial distance of the density to the above solar wind/magnetospheric quantity.

Figure S5.

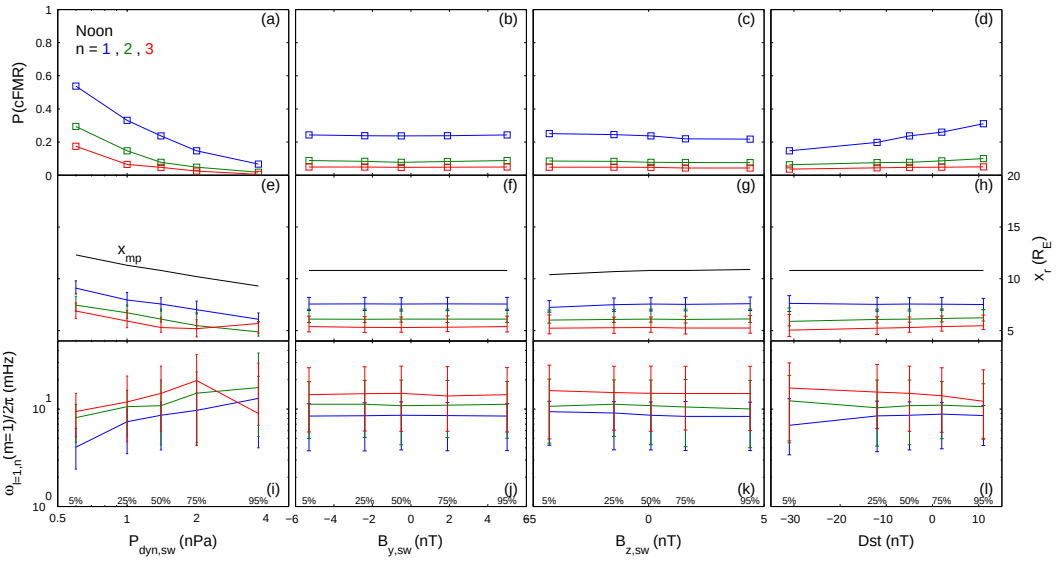

Variation of noon cFMR occurrence probability (a–d), resonance location (e–h) and frequency (i–j) with T96 inputs at their respective 5th, 25th, 50th, 75th and 95th percentiles. Medians (lines) and interquartile ranges (error bars) are displayed for $n = 1$–3 (blue, green, red). The magnetopause location is shown for reference as the black lines in e–h.

Table S6.

Index	Noon	
	a	b
$\max(Kp)_{36h}$	-2.0	12.7
$\log_{10}[\max(AE)_{36h}]$	-10.3	33.1
$\log_{10}[-\min(Dst)_{36h}]$	-15.3	26.6

Linear fit coefficients to the inner boundary location with activity

References

O'Brien, T. P., and M. B. Moldwin, Empirical plasmapause models from magnetic indices, *Geophys. Res. Lett.*, *30*, 1152, 2003.